FORCED VIBRATION: AXIALLY FUNCTIONALLY GRADED THIN BEAMS ON ELASTIC FOUNDATION

Anoop Bahuguna[1], Ajay Kumar Singh[2], Kishan Singh Rawat[3]

[1]Department of Civil Engineering, Graphic Era Deemed to be University, Dehradun, Uttarakhand India
[2]Department of Civil Engineering, Graphic Era Hill University, Uttarakhand India
[3]Department of Civil Engineering, Graphic Era Hill University, Uttarakhand India

ABSTRACT

The member susceptible to loads is supported on continuous elastic foundations such as soil or flowable fill in some applications, such as grade beams in prefabricated buildings and combined footings for industrial tanks and equipment. In other words, the member's length is dispersed with the responses brought on by external loading. The loads are factored and can be found from equipment vendor loading data or building column reactions, and this shows a generic footing and load data. In this illustration, the loads span the entire width of the footing and come from horizontal tank supports. The Reference's finite element analysis results are contrasted with those from StructurePoint's spBeam engineering software tool.

Keywords: industrial tanks, beams, elastic foundation, column, external loading

INTRODUCTION

Forced vibration analysis can be defined as the study of the dynamic behaviour of structural parts under time-varying external force or excitation. Such dynamic loading circumstances are typically produced in engineering applications by spinning machinery that is unbalanced, forces generated by reciprocating machinery, or machine motion. A typical illustration of a dynamic loading condition is harmonic excitation,[1–5] which refers to forces that change harmonically throughout time. Pure harmonic excitation is less likely to happen in a working environment than periodic or other types of excitation[6–10], but it is important to understand how a system behaves under harmonic excitation to understand how the system will react to more general types of excitation. It is also acknowledged that a system may respond to harmonic stimuli in a periodic, non-harmonic manner. However, in the current situation, it is expected that harmonic excitation will result in a harmonic response of the same frequency, therefore such conditions are not taken into consideration.

[11-13] The system currently being considered is the same as that which is detailed it depicts a different perspective of the system (compared to those in the previous chapter) and lists the system's geometrical and material parameters. [14-15]The beam's undeformed state and deflected configuration by transverse external excitation are shown in the figure. The length L of the tapered AFG beam rests on a linear elastic base. The cross-sectional dimensions are represented by the variables b(x) and t. (x). The longitudinal axis is the direction of the material are graded. The

stiffness of the foundation is assumed to be K, and its impact on the system is taken into account in terms of a string of linear springs with the same stiffness coefficient as the foundation (Fig. 1). Although the formulation can undoubtedly manage taper in either thickness or breadth singly or together, the thickness variation is not shown in this illustrative figure.
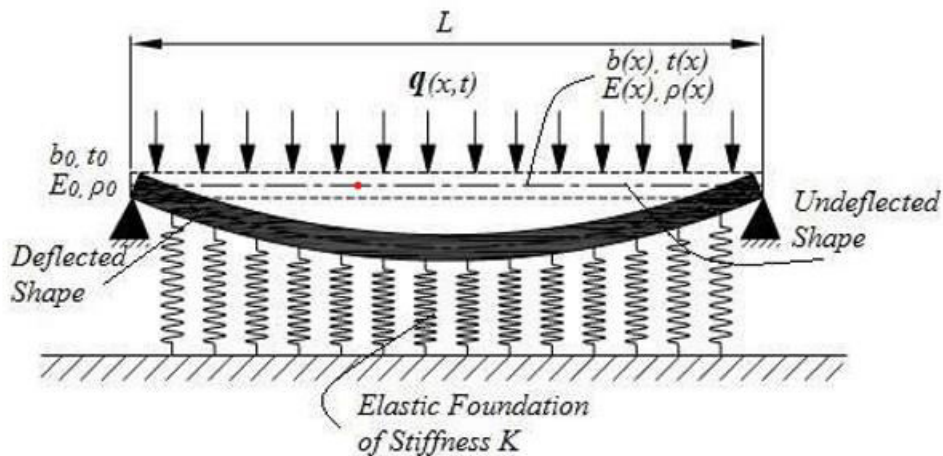

Figure 1: a succession of linear representations of an AFG beam supported on an elastic basis

Results and discussions:
The expression q * = q(L4/ E0I0t0) makes the harmonic excitation's intensity, q, dimensionless. In the current investigation, q * is altered from 30 to 60 in a 10-fold range. However, the above equation can also be substituted with the numerical stydy of any type of pattern of excitation. For each taper pattern, four alternative taper parameter values are taken into account here, and these values are displayed. Gradations in elastic modulus and density are taken into account while analysing material quality variations along the length of the beam. In this chapter, three distinct models for these two material parameter variations are described.

Convergence study:
Using the Gram-Schmidt orthogonalization concept, these chosen start functions are utilized to produce higher order functions. The number of higher order functions that should be constructed for w and u is a crucial decision. The precision of the results produced is also significantly influenced by the number of Gauss points (ng). Therefore, it is necessary to do the required convergence tests in order to determine appropriate values for these parameters. A clamped beam with a parabolic profile and a taper parameter of 0.2 is the subject of the convergence investigation. The beam is supported by an elastic base with a stiffness of K = 103 N/m. The material model used in this investigation is referred to as model 2. Figure 2 displays the convergence study's findings. Figure 2 plots the system's normalised maximum deflection (wmax/t0) vs the quantity of Gauss points (ng) (a). From this research, 24 Gauss points are selected for the current task.
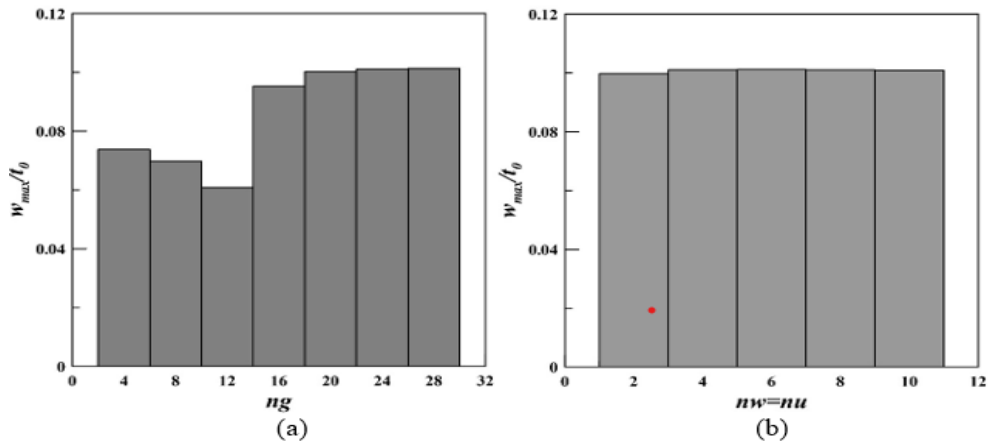
Figure 2: a study of convergence for the number of orthogonal functions and the number of gauss points

Validation study:

The next step is to determine whether the current methodology and solution technique are valid once the parameter values listed above that correspond to the numerical scheme have been determined.

Stiffness of foundation effect:

Figures 3 depict the frequency response of a linearly tapered beam on an elastic foundation using three different material types . Four response curves for a range of spring stiffness values from 2 to 28 are shown in each of the three sets of plots for three different boundary conditions that are present in each image. The taper parameter is held constant at 0.4 so that the results can be shown and the impacts of the foundation stiffness may be studied.
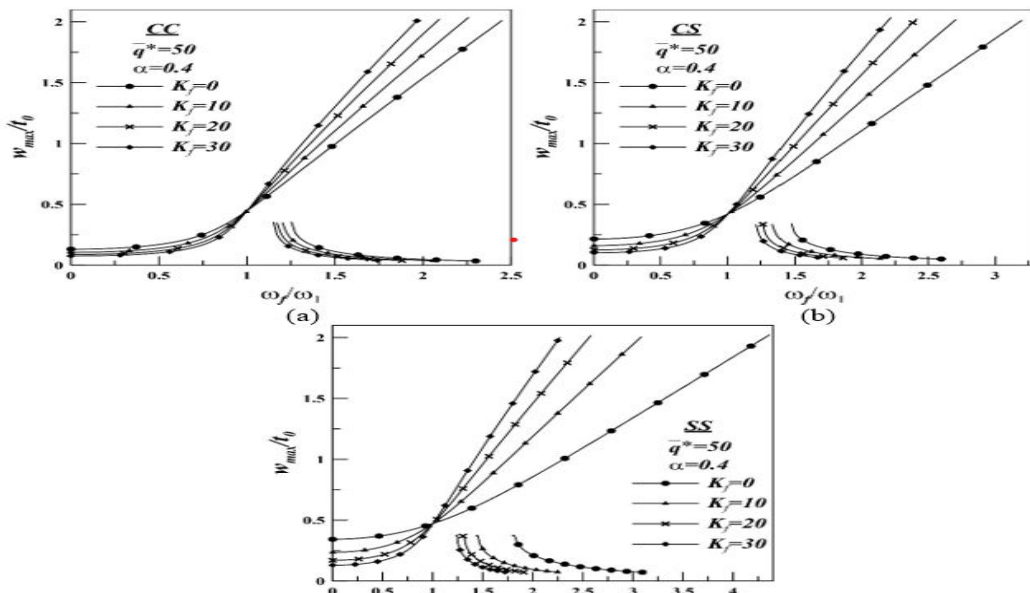

Figure 3: AFG parabolic taper beam frequency response (Material 3) for various boundary conditions: (a) CC (b), (c), and SS

With a change in the foundation stiffness, these sets of plots would have produced four distinct backbone curves, and including them all in one figure would have made it crowded. Therefore, a deliberate choice is made not to include these system foundations in order to preserve the accuracy of the numbers.
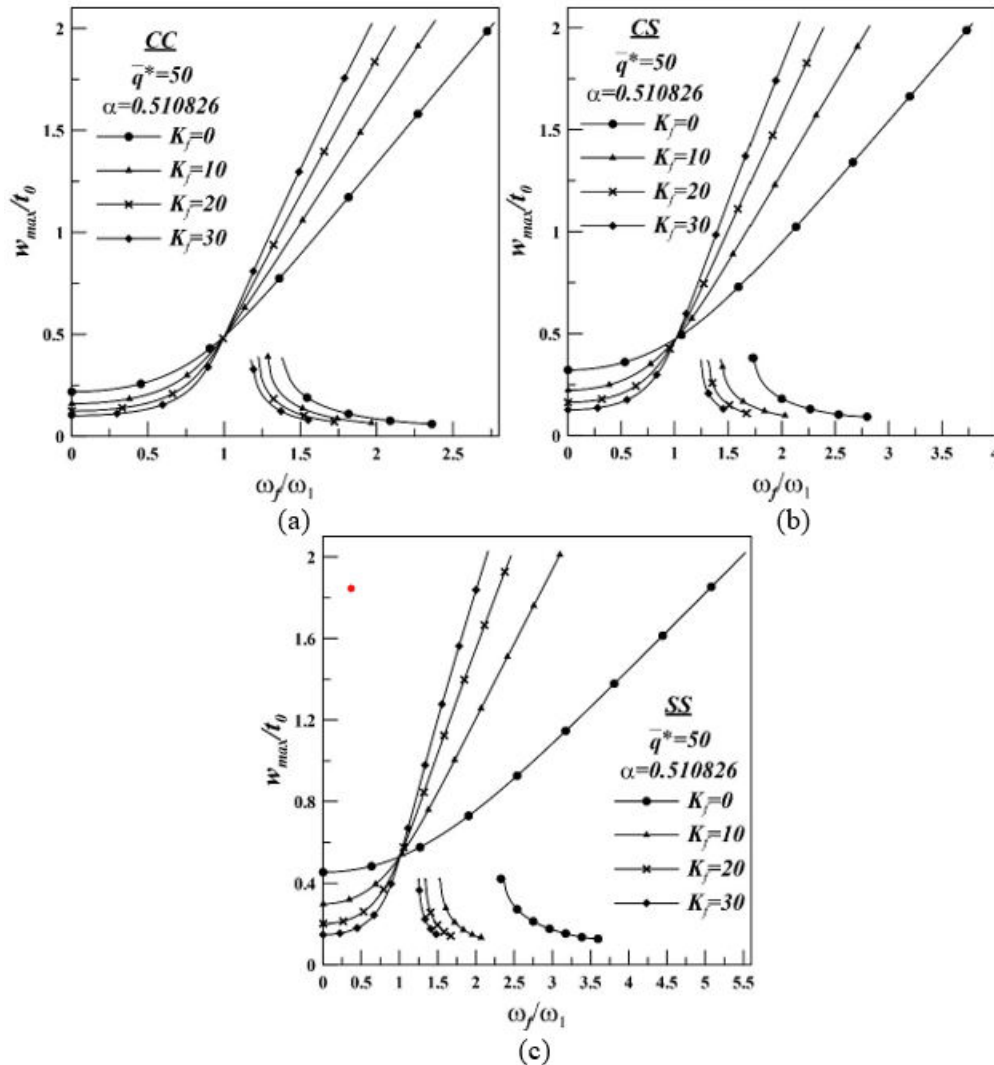

Figure 4: AFG exponential taper beam's frequency response under various boundary conditions: (a) CC (b) CS & SS (c)

Figures 5 show that the response amplitude always falls in the low excitation frequency zone as the foundation stiffness increases. It is clear from the description above that the SS beam has stronger nonlinearity than the other two taper patterns. The difference in the response curves for CC and CS beam is found to be minimal.
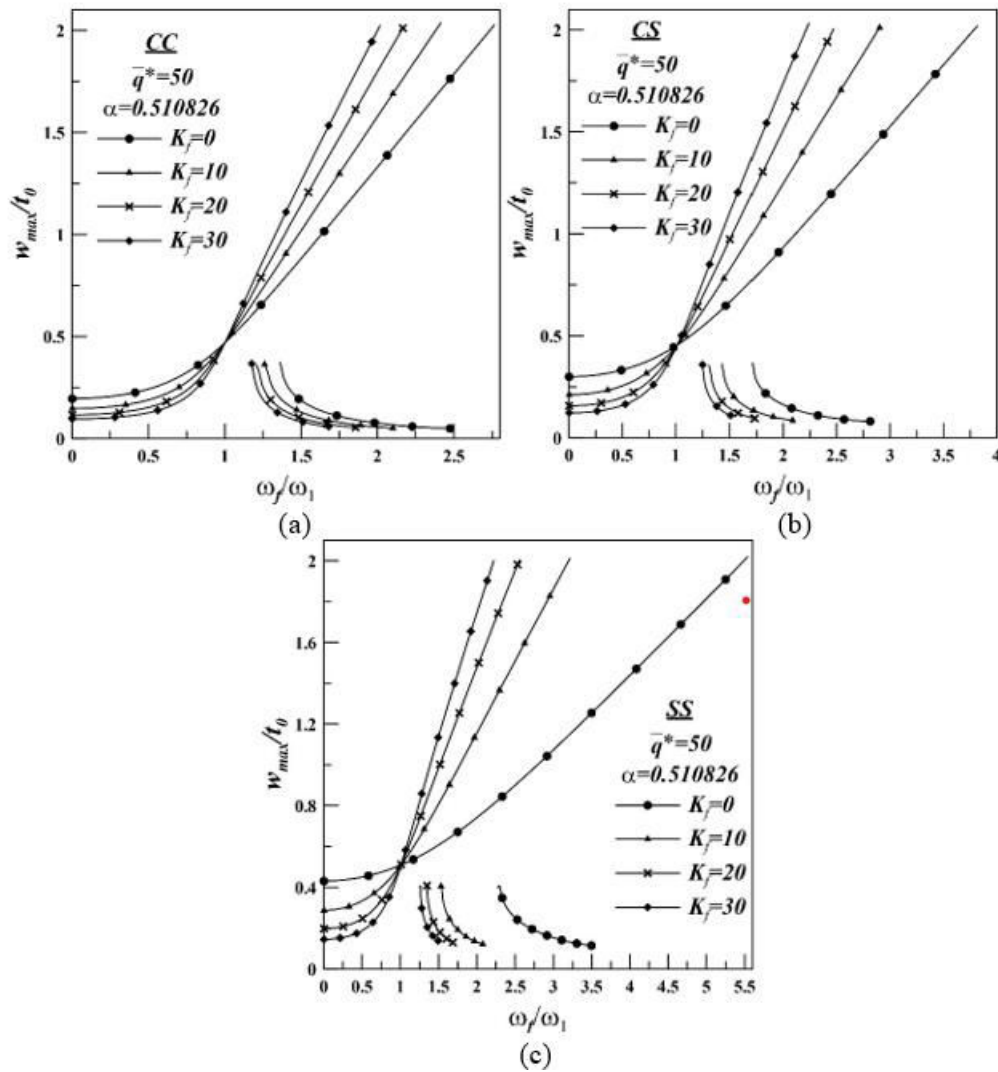
Figure 5: AFG exponential taper beam's frequency response under various boundary conditions (Material 3): (a) CC (b) CS & SS (c)

The variation in response curves for various material models for a given example of boundary condition is infrequently found for linear taper patterns, as demonstrated in Figures 4.5–4.7. The similar pattern may be seen for different types of taper patterns, such as parabolic and exponential taper. Additionally, it can be seen from the figures that for a specific boundary

For various foundation stiffness values, the reaction curves in the exponential taper are more visibly grouped than those in the other two (linear and parabolic).
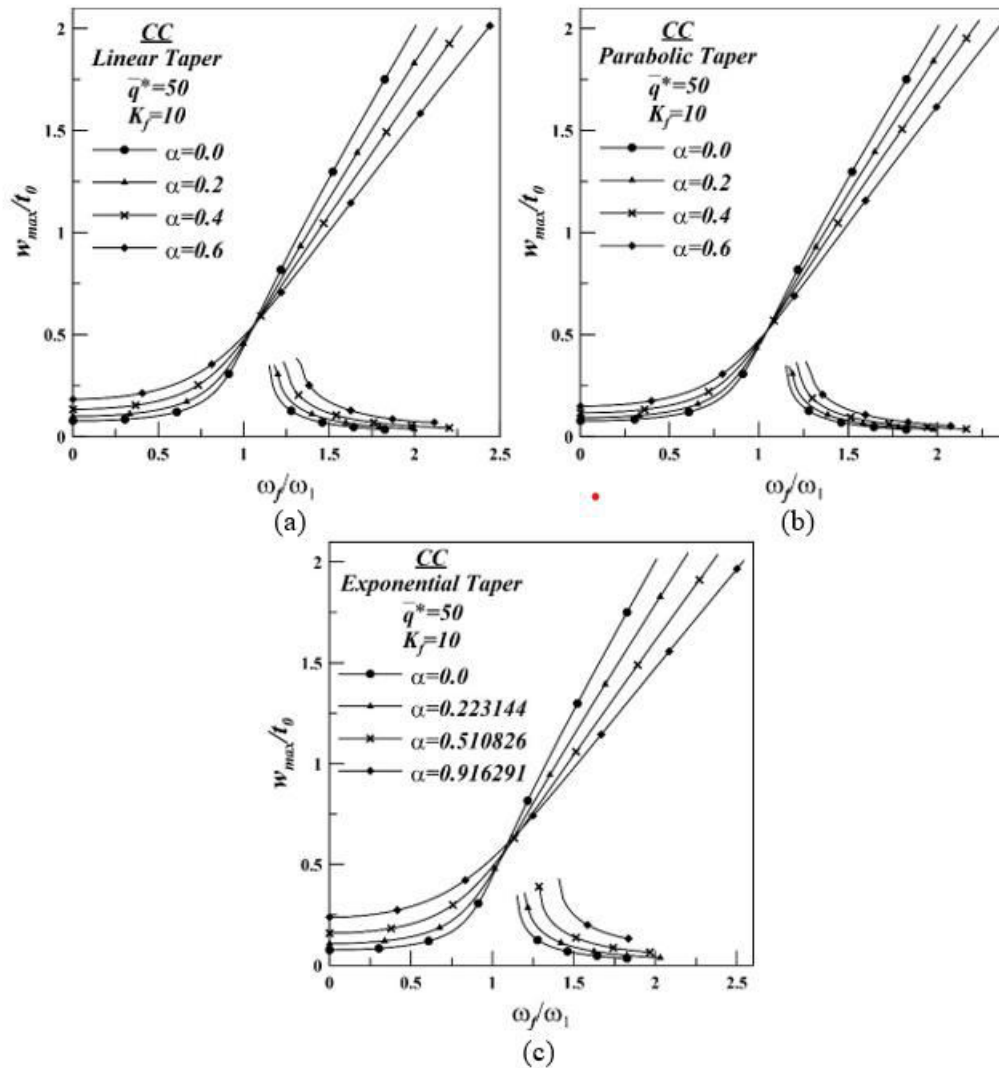
Fig. 6: Effects of the taper parameter for (a) linear taper, (b) parabolic taper, and (c) exponential taper on the frequency response for CC beam

Effect of tapering:
Figure 7 illustrates how the taper parameter affects the forced vibration response of the AFG Timoshenko beam for different boundaries. Three different taper patterns are considered when the CC border condition is taken into account. While the numbers for linear and parabolic taper patterns' taper parameters range from 0 to 0.6, those for exponential taper patterns' taper parameters range from 1 to 1.87535. It should be noted that the case of a uniform beam is represented by the taper value of 0.0. The foundation stiffness and excitation amplitude have been set to 50 and 10, respectively. Figure 7 demonstrates that the response's amplitude increases naturally in the low frequency domain when taper parameter values increase, whereas the trend This pattern of elimination of material with increasing taper, which further reduces the rigidity of the beam, is observed. For the sake of greater clarity, the backbone curves for the four distinct scenarios are not included in these sets of figures.
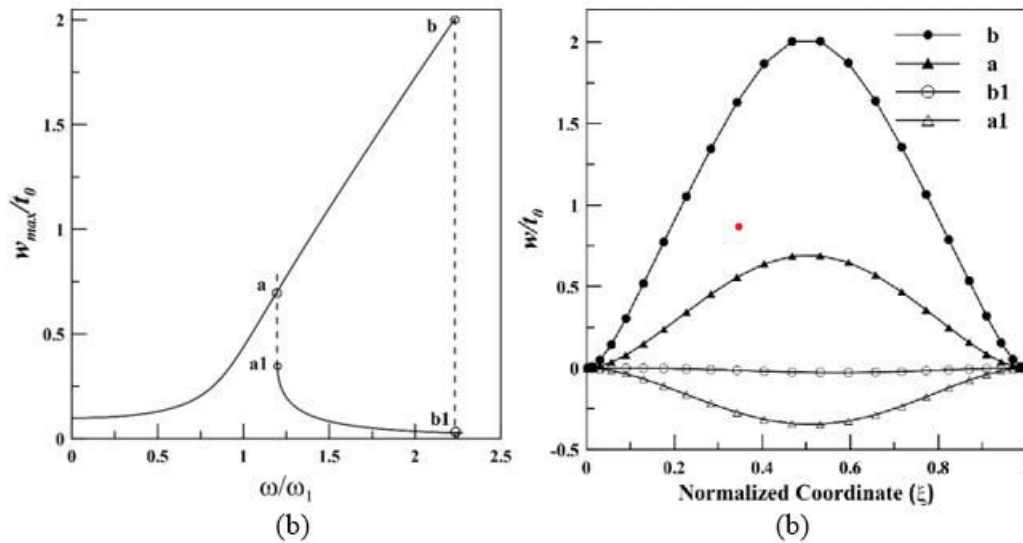Operational deflected shape (ODS):

Fig 7 ODS plot

The Material model 2 is taken into consideration, and the beam is supported by a base with a rigidity of 103 N/m. The frequency-response curve and a few typical points are shown in Figure 8(a). Figure 8 displays the ODS corresponding to these typical sites (b). Despite having a varying maximum response amplitude, the ODS of various example locations appears to be identical.

Conclusion

The set of governing equations also displays nonlinear characteristics as a result of taking into account nonlinear strain-displacement interactions. The set of nonlinear equations are solved using Broyden's method, and numerical results in terms of longitudinal and in-plane motion fields are discovered. The current strategy and solution process are validated by results from earlier literature that have been established. FRC are employed in non-dimensional stimulation frequency-maximum reaction amplitude charts to depict the geometrically nonlinear forced vibration property of the system. New results that can be used as benchmark results are presented for a set of four flexural boundary conditions, 3 material models, and 4 foundation stiffness values. However, because the formulation and solution technique is so generic, it can handle other types of taper patterns, material gradations, and excitation patterns with little alterations.

Reference:
1. Vinyas, M., and Subhas Chandra Kattimani. "Static studies of stepped functionally graded magneto-electro-elastic beam subjected to different thermal loads." Composite Structures 163 (2017): 216-237.
2. Vinyas, M., and Subhas Chandra Kattimani. "Static behavior of thermally loaded multilayered magneto-electro-elastic beam." (2017).
3. Kasivitamnuay, Jirapong, and Pairod Singhatanadgid. "Scaling laws for displacement of elastic beam by energy method." International Journal of Mechanical Sciences 128 (2017): 361-367.
4. Romano, Giovanni, et al. "Constitutive boundary conditions and paradoxes in nonlocal

elastic nanobeams." International Journal of Mechanical Sciences 121 (2017): 151-156.

5. Vinyas, M., and Subhas Chandra Kattimani. "A 3D finite element static and free vibration analysis of magneto-electro-elastic beam." (2017).

6. Li, Fengming, Chuanzeng Zhang, and Chunchuan Liu. "Active tuning of vibration and wave propagation in elastic beams with periodically placed piezoelectric actuator/sensor pairs." Journal of Sound and Vibration 393 (2017): 14-29.

7. Ebrahimi, F., and M. R. Barati. "Buckling analysis of smart size-dependent higher order magneto-electro-thermo-elastic functionally graded nanosize beams." Journal of Mechanics 33.1 (2017): 23-33.

8. Demir, Çiğdem, and Ömer Civalek. "A new nonlocal FEM via Hermitian cubic shape functions for thermal vibration of nano beams surrounded by an elastic matrix." Composite Structures 168 (2017): 872-884.

9. Vinyas, M., and Subhas Chandra Kattimani. "A finite element based assessment of static behavior of multiphase magneto-electro-elastic beams under different thermal loading." (2017).

10. Refaeinejad, V., O. Rahmani, and S. A. H. Hosseini. "An analytical solution for bending, buckling, and free vibration of FG nanobeam lying on Winkler-Pasternak elastic foundation using different nonlocal higher order shear deformation beam theories." Scientia Iranica 24.3 (2017): 1635-1653.

11. Chen, Yangyang, Gengkai Hu, and Guoliang Huang. "A hybrid elastic metamaterial with negative mass density and tunable bending stiffness." Journal of the Mechanics and Physics of Solids 105 (2017): 179-198.

12. Ebrahimi, Farzad, and Mohammad Reza Barati. "Buckling analysis of nonlocal third-order shear deformable functionally graded piezoelectric nanobeams embedded in elastic medium." Journal of the Brazilian Society of Mechanical Sciences and Engineering 39.3 (2017): 937-952.

13. Lim, Tae-Kyung, and Ji-Hwan Kim. "Thermo-elastic effects on shear correction factors for functionally graded beam." Composites Part B: Engineering 123 (2017): 262-270.

14. Wang, Hui, et al. "Experimental and theoretical analyses of elastic-plastic repeated impacts by considering wave effects." European Journal of Mechanics-A/Solids 65 (2017): 212-222.

15. Al-Dahawi, Ali, et al. "Assessment of self-sensing capability of Engineered Cementitious Composites within the elastic and plastic ranges of cyclic flexural loading." Construction and Building Materials 145 (2017): 1-10.